19,10,04

Heat Capacity of Scandoborate $NdSc_3(BO_3)_4$

© E.V. Eremin[1,2,3], N.D. Andryushin[1,2], I.A. Gudim[1], M.S. Pavlovskii[1,2], V.R. Titova[1,2]

[1] Kirensky Institute of Physics, Federal Research Center KSC SB, Russian Academy of Sciences, Krasnoyarsk, Russia
[2] Siberian Federal University, Krasnoyarsk, Russia
[3] Siberian State University of Science and Technology, Krasnoyarsk, Russia

E-mail: eev@iph.krasn.ru

Received August 11, 2021
Revised August 11, 2021
Accepted August 20, 2021

Single crystals of trigonal neodymium scandoborate $NdSc_3(BO_3)_4$ were grown by the group method from a solution-melt based on bismuth trimolybdate. The molar heat capacity $C(T)$ was studied in the temperature range 2–300 K and magnetic fields up to 9 T. The experimental curve was approximated by the combined Debye–Einstein model. The lattice contribution was determined from ab-initio calculations. Schottky anomaly was observed in the low-temperature region $C(T)$ with the applied magnetic field.

Keywords: crystal growth, magnetoelectrics, heat capacity, Schottky anomaly.

DOI: 10.21883/PSS.2022.14.54353.188

1. Introduction

Trigonal rare earth oxyborates $ReM_3(BO_3)_4$ (*Re* — rare earth ion, M = Al, Sc, Fe, Ga) are actively studied during the last decade due to multiple options of various combinations of *Re* and *M* elements and, consequently, large variety of physical properties [1–8]. Oxyborates have rhombohedral structure of natural mineral huntite type, described with spatial group R32 or $P3_121$. Non-centrosymmetric structure makes these materials the great candidates for optical applications due to their good luminescent and non-linear optical properties. For ferroborates $ReFe_3(BO_3)_4$ their belonging to a new class of multiferroics is established, where magnetic, electric and elastic ordering parameters coexist.

Interest to paramagnetic alumoborates increased with revealing of large magnetoelectric effect in $TmAl_3(BO_3)_4$ [9], that is comparable in value to the observed effects in isostructural ferroborates $ReFe_3(BO_3)_4$. Later even larger magnetoelectric effect was revealed in $HoAl_3(BO_3)_4$ [10], which value exceeds known maximum values of magnetoelectric polarization in ferroborates in several times [3,5]. Increase of magnetoelectric effect is also observed at substitution of Fe^{3+} ions in $HoFe_3(BO_3)_4$ with Ga^{3+} ions [11].

Considering, that at substitution of magnetic subsystem (Fe) in $ReM_3(BO_3)_4$ with non-magnetic (Al,Ga) the magnetoelectric effect reaches gigantic values, there is an interest also to study other subclasses or oxyborates with huntite structure with single magnetic subsystem, for instance, rare earth scandoborates $ReSc_3(BO_3)_4$. The structural [12] and magnetic and magnetoelectric properties [13] were already studied in neodymium scandoborate. But little is known about its thermodynamic properties, which are the subject of this study.

2. Preparation of samples and measurement procedure

Monocrystals of $NdSc_3(BO_3)_4$ were grown from a solution-melt based on bismuth trimolybdate as per technology, described in detail in the work [14]. Heat capacity was measured using PPMS QuantumDesign setup (Common Use Center of the Federal Research Center „Krasnoyarsk Science Center of the Siberian Branch of the Russian Academy of Sciences“) in temperature range from 2 to 300 K and magnetic fields of up to 9 T. Relative accuracy of data was above 1% in the whole temperature range.

First-principles calculations were performed using plane augmented wave (PAW) method [15] within the framework of the density functional theory (DFT), implemented in the VASP software package [16,17]. Generalized gradient approximation (GGA) functional with PBE parametrization was used [18]. Plane waves energy was limited with 600 eV. Grid in k-space for Brillouin zone was built as per Monkhorst–Pack scheme [19] and had dimensions of $7 \times 7 \times 7$. Dynamic lattice calculations were performed for calculation of a lattice heat capacity. During calculation a supercell was built ($2 \times 2 \times 2$) and force constants calculation was performed using small shifts method, implemented in PHONOPY [20].

3. Results and discussion

Earlier it was revealed, that at high temperature $NdSc_3(BO_3)_4$ has rhombohedral structure, described with spatial group R32, and with temperature lowering (T_s = 504 K) the structure transition $R32 \rightarrow P3_121$ is ob-

served [12]. It was also demonstrated, that magnetically $NdSc_3(BO_3)_4$ is a paramagnetic, which properties are completely defined with magnetic behavior of Nd^{3+} ion [13].

Figure 1 shows results of measurement of molar heat capacity $C(T)$ in a temperature range of 2–300 K. It is seen, that values of $C(T)$ grow with temperature increase without any anomalies, thus indicating the lack of magnetic and structural transitions in the examined range.

The obtained curve is well approximated with a combined Debye–Einstein model:

$$C(T) = x \cdot 9nR\left(\frac{T}{\theta_D}\right)^3 \int_0^{\theta_D/T} \frac{t^4 \exp(t)}{\left(\exp(t)-1\right)^2}\, dt + (1-x)\cdot 3nR\left(\frac{\theta_E}{T}\right)^2 \frac{\exp(\theta_E/T)}{\left(\exp(\theta_E/T)-1\right)^2}, \quad (1)$$

where θ_D — Debye temperature (obtained value $\theta_D = 382.61$ K) and θ_E — Einstein temperature (obtained value $\theta_E = 991.64$ K) (Fig. 2). Parameters x and $(1-x)$ define a share of Debye and Einstein model respectively (after approximation it was 49.1% of Debye and 50.9% of Einstein). It should be noted, that molar heat capacity of adjusting dependence does not exceed classical limit of Dulong–Petit of $3Rn$, where R — universal gas constant, and n — number of atoms in formula unit of $NdSc_3(BO_3)_4$ ($n = 20$).

For comparison the first-principles calculations of lattice contribution to heat capacity were performed, and the contribution was calculated from the following expression:

$$C(T) = \left(\frac{\partial E}{\partial T}\right)_V = \sum_{qv} k_B\left(\hbar\omega(qv)/k_BT\right)^2 \times \frac{\exp\left(\hbar\omega(qv)/k_BT\right)}{\left(\exp(\hbar\omega(qv)/k_BT)-1\right)^2}, \quad (2)$$

where $\omega(qv)$ — frequency of phonon mode with wave vector q and number of branch v.

Since at phase transition $R32 \rightarrow P3_121$ the tripling of a lattice cell is observed in crystals with huntite structure, in terms of calculation time saving it is preferable to perform calculations of lattice dynamics in a more symmetrical phase R32, containing 20 atoms in lattice cell, than in phase $P3_121$, containing 60 atoms in lattice cell. The main structural features at phase transition $R32 \rightarrow P3_121$ remain, and it can be expected, that lattice contribution to heat capacity in these two phases will be qualitatively equal. From the other side, presence of imaginary modes in $NdSc_3(BO_3)_4$ in phase R32 prevents from accurate calculation of the lattice heat capacity, see formula (2). Therefore, a diamagnetic analogue of $LaSc_3(BO_3)_4$ with spatial symmetry group R32 was selected as an object, in which, as seen from the calculation, the structural instabilities are not observed and all phonon modes are stable. Thus calculation results are shown in Fig. 2. There is a good agreement of theory and experiment, that indicates correctness of the selected model.

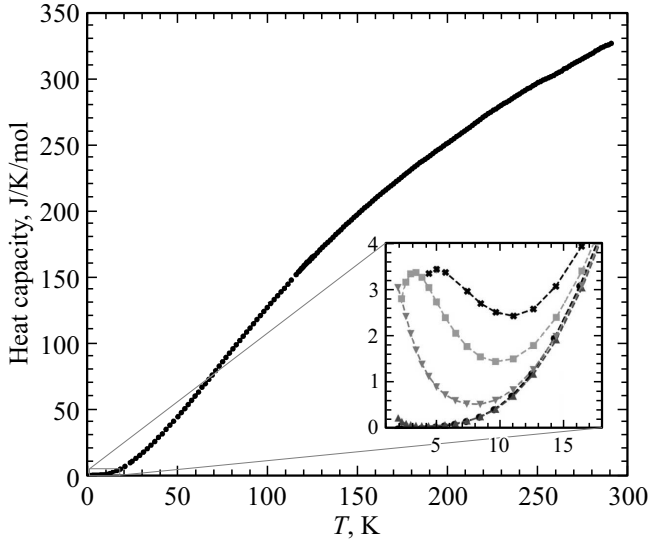

Figure 1. Molar heat capacity of $NdSc_3(BO_3)_4$ is about 2–300 K. In insert the heat capacity is in low-temperatures region: circles — without field, triangles looking upward — field of 1 T, triangles looking downward — field of 3 T, squares — 6 T, crosses — 9 T.

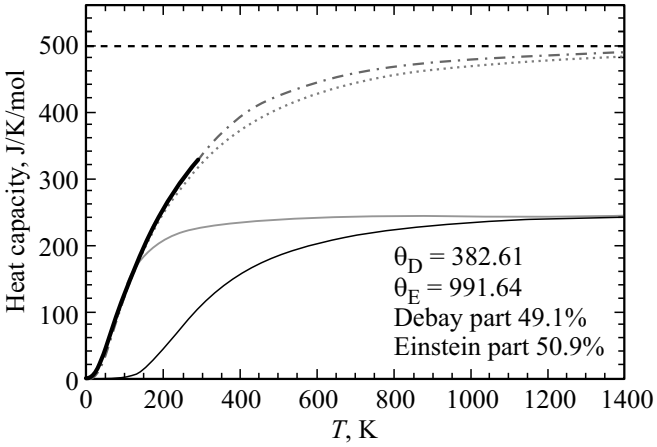

Figure 2. Dependence of molar heat capacity on temperature. Large black dots — experimentally obtained heat capacity of $NdSc_3(BO_3)_4$, dot-and-dash curve — approximation of experimental data in the combined Debye and Einstein model. Grey and black thin solid lines — parts of approximation, relating to Debye and Einstein models respectively. Small grey dots — heat capacity of $LaSc_3(BO_3)_4$, obtained from the first-principles calculations. Black dashed line corresponds to Dulong–Petit law.

At application of magnetic field, directed along the third order axis (c-axis), the Schottky anomaly is observed in the low-temperature region, which shifts towards high-temperature region with magnetic field increase (insert in Fig. 1). This anomaly appears due to splitting of the ground doublet of Kramers ion of Nd^{3+} in magnetic field, and, as a result, redistribution of this doublet level population.

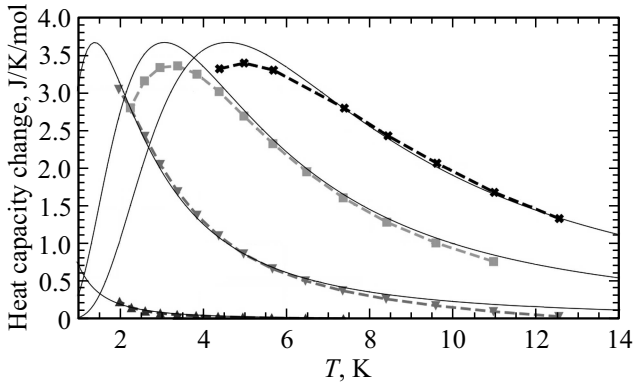

Figure 3. Change of low-temperature heat capacity in $NdSc_3(BO_3)_4$ at application of external field: triangles looking upward — field of 1 T, triangles looking downward — field of 3 T, squares — 6 T, crosses — 9 T. Solid curves are obtained using approximation of experimental data.

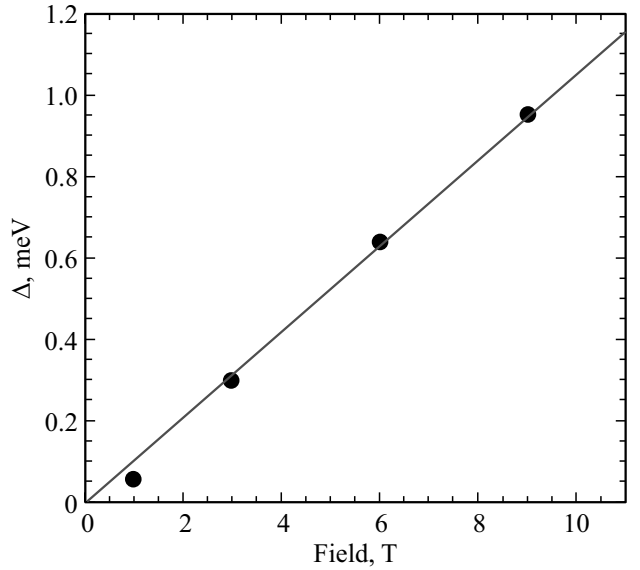

Figure 4. Dependence of energy between two levels on external field. Solid line is obtained from approximation with linear function.

For two-level system the heat capacity from Schottky anomaly is the following

$$C(T) = \left(\frac{\partial E}{\partial T}\right)_{\Delta} = k_{\mathrm{B}} \frac{(\Delta/T)^2 \exp(\Delta/T)}{\left(1+\exp(\Delta/T)\right)^2}, \qquad (3)$$

where Δ — energy between two levels.

Figure 3 shows the calculated contribution of rare-earth subsystem to heat capacity in magnetic fields of 1, 3, 6 and 9 T. The figure shows good agreement of theory and experiment.

Figure 4 shows dependence of adjusting parameter Δ on magnetic field value. This dependence is linear, as it should be as per formula (3).

Two-level system of the ground doublet of neodymium ion of Nd^{3+} ($^4I_{9/2}$) can be described with spin Hamiltonian with effective spin $S = 1/2$ and anisotropic g-tensor with axial symmetry [21]:

$$\mathscr{H} = g_{\parallel} S_z H_z \cdot \mu_{\mathrm{B}} + g_{\perp}(S_x H_x + S_y H_y) \cdot \mu_{\mathrm{B}}, \qquad (4)$$

where $g_{\parallel}, g_{\perp}$ — g-factor of Nd^{3+} ion in magnetic field orientation parallel and perpendicular to c-axis respectively, S_x, S_y, S_z — projections of a spin mechanical moment to quantization axes, μ_{B} — Bohr magneton.

Excited level energy is equal to Δ value. From linear dependence $\Delta(T)$ from Fig. 4 in geometry of $H \parallel c$ it is easy to define, that $g_{\parallel} S_z = 1.82\,\mu_{\mathrm{B}}$, from where it can be obtained, that $g_{\parallel} = 3.64$.

4. Conclusion

Scandoborate $NdSc_3(BO_3)_4$ was grown from a solution-melt based on bismuth trimolybdate using the group method. Its caloric properties in the temperature range of 2–300 K and magnetic field of up to 9 T were studied for the first time.

Within the examined temperature range there is no anomalies on dependence $C(T)$, indicating magnetic or structural transitions. Experimental curve was approximated with the combined Debye–Einstein model, Debye temperature $\theta_{\mathrm{D}} = 991.64$ K and Einstein temperature $\theta_{\mathrm{E}} = 382.61$ K were determined.

The first-principles calculations of the lattice contribution of $NdSc_3(BO_3)_4$ were performed. For that the diamagnetic analogue — isostructural compound of $LaSc_3(BO_3)_4$ was selected as the object. The good agreement of theory and experiment was obtained.

At application of magnetic field, directed along c-axis in the low-temperature region the Schottky anomaly was observed, which shifts towards high-temperature region with magnetic field increase. Two-level system of the ground doublet of neodymium ion of Nd^{3+} ($^4I_{9/2}$) was described with spin Hamiltonian with effective spin $S = 1/2$. In this model the g-factor in geometry of $B \parallel c$ ($g_{\parallel} = 3.64$) was defined.

Funding

The study was done with financial support from the Russian Foundation for Basic Research, Government of Krasnoyarsk Territory and the Krasnoyarsk Regional Fund of Science within the scientific project „Development of solution-melt technologies of growing the new monocrystals of $NdSc_{3-x}Ga_x(BO_3)_4$ with huntite structure and study of interaction of their magnetic, electric and elastic subsystems“ (No. 20-42-240009).

Conflict of interest

The authors declare that they have no conflict of interest.

References

[1] A.K. Zvezdin, S.S. Krotov, A.M. Kadomtseva, G.P. Vorob'ev, Yu.F. Popov, A.P. Pyatakov, L.N. Bezmaternykh, E.A. Popova. Pis'ma v ZhETF **81**, *6*, 335 (2005) (in Russian).
[2] E.A. Popova, D.V. Volkov, A.N. Vasiliev, A.A. Demidov, N.P. Kolmakova, I.A. Gudim, L.N. Bezmaternykh, N. Tristan, Yu. Skourski, B. Buechner, C. Hess, R. Klingeler. Phys. Rev. B **75**, *22*, 224413 (2007).
[3] R.P. Chaudhury, F. Yen, B. Lorenz, Y.Y. Sun, L.N. Bezmaternykh, V.L. Temerov, C.W. Chu. Phys. Rev. B **80**, *10*, 104424 (2009).
[4] A.M. Kadomtseva, Yu.F. Popov, G.P. Vorob'ev, A.P. Pyatakov, S.S. Krotov, K.I. Kamilov, V.Yu. Ivanov, A.A. Mukhin, A.K. Zvezdin, A.M. Kuzmenko, L.N. Bezmaternykh, I.A. Gudim, V.L. Temerov. FNT **36**, *6*, 640 (2010) (in Russian).
[5] V.I. Zinenko, M.S. Pavlovskiy, A.S. Krylov, I.A. Gudim, E.V. Eremin. ZhETF **144**, *6*, 1174 (2013) (in Russian).
[6] A.P. Pyatakov, A.K. Zvezdin. UFN **182**, *6*, 593(2012) (in Russian).
[7] A.N. Vasiliev, E.A. Popova. FNT **32**, *8/9*, 968 (2006) (in Russian).
[8] T. Usui, Y. Tanaka, H. Nakajima, M. Taguchi, A. Chainani, M. Oura, S. Shin, N. Katayama, H. Sawa, Y. Wakabayashi, T. Kimura. Nature Mater. **13**, *6*, 611 (2014).
[9] R.P. Chaudhury, B. Lorenz, Y.Y. Sun, L.N. Bezmaternykh, V.L. Temerov, C.W. Chu. Phys. Rev. B **81**, *22*, 220402 (R) (2010).
[10] K.-C. Liang, R.P. Chaudhury, B. Lorenz, Y.Y. Sun, L.N. Bezmaternykh, V.L. Temerov, C.W. Chu. Phys. Rev. B **83**, *18*, 180417 (2011).
[11] N.V. Volkov, I.A. Gudim, E.V. Eremin, I.A. Begunov, A.A. Demidov, K.N. Boldyrev. Pis'ma v ZhETF **99**, *2*, 72 (2014) (in Russian).
[12] E.V. Eremin, M.S. Pavlovskiy, I.A. Gudim, V.L. Temerov, M.S. Molokeev, N.D. Andryushin, E.V. Bogdanov. J. Alloys Compd. **828**, 154355 (2020).
[13] E.V. Eremin, A.A. Dubrovsky, I.A. Gudim, V.R. Titova, M.V. Merkulov. FTT **63**, *7*, 911 (2021) (in Russian).
[14] L.N. Bezmaternykh, V.L. Temerov, I.A. Gudim, N.A. Stolbovaya. Crystallogr. Rep. **50**, *1*, S97 (2005).
[15] G. Kresse, D. Joubert. Phys. Rev. B **59**, *3*, 1758 (1999).
[16] G. Kresse, J. Furthmüller. Phys. Rev. B **54**, *16*, 11169 (1996).
[17] G. Kresse, J. Furthmüller. Comput. Mater. Sci. **6**, *1*, 15 (1996).
[18] J.P. Perdew, K. Burke, M. Ernzerhof. Phys. Rev. Lett. **77**, *18*, 3865 (1996).
[19] H.J. Monkhorst, J.D. Pack. Phys. Rev. B **13**, *12*, 5188 (1976).
[20] A. Togo, T. Tanaka. Scripta Mater. **108**, 1 (2015).
[21] A. Abragam, B. Blini. Elektronnyj paramagnitnyj rezonans perekhodnykh ionov. Mir, M. (1972). T. 1. 651 p. (in Russian).

Editor E.V. Tolstyakova